Microbial cell viability-driven operational strategy for enhanced acetate production in syngas fermentation

Lee, Mungyu; Kim, Ji Yeon; Ji, Nulee; Jourdin, Ludovic; Straathof, Adrie J.J.; Chang, In Seop

DOI
10.1016/j.jece.2025.116531

Publication date
2025

Document Version
Final published version

Published in
Journal of Environmental Chemical Engineering

Journal of Environmental Chemical Engineering 13 (2025) 116531

Contents lists available at ScienceDirect

Journal of Environmental Chemical Engineering

journal homepage: www.elsevier.com/locate/jece

Microbial cell viability-driven operational strategy for enhanced acetate production in syngas fermentation

Mungyu Lee [a,c], Ji-Yeon Kim [a,b], Nulee Ji [a], Ludovic Jourdin [c], Adrie J.J. Straathof [c], In Seop Chang [a,b,*]

[a] School of Environment and Energy Engineering, Gwangju Institute of Science and Technology, 123 Cheomdan-gwagiro, Buk-gu, Gwangju 61005, Republic of Korea
[b] Research Center for Innovative Energy and Carbon Optimized Synthesis for Chemicals (Inn-ECOSysChem), Gwangju Institute of Science and Technology, Gwangju 61005, Republic of Korea
[c] Department of Biotechnology, Delft University of Technology, van der Maasweg 9, Delft 2629 Hz, the Netherlands

ARTICLE INFO

Keywords:
Carbon conversion
Gas fermentation
Cell viability
Specific productivity
Viable cell

ABSTRACT

Syngas fermentation is a promising bioprocessing method that utilises autotrophic organisms to convert C1 gases, such as CO and CO_2, into valuable chemicals, offering both environmental and economic benefits. Despite these advantages, the industrial application of gas fermentation remains limited owing to challenges in productivity associated with gas substrates. While previous studies have focused on optimizing reactor design, mass transfer, and growth medium as solutions to these specific challenges, the direct correlation between cell viability and productivity remains unexplored. To address this gap, this study investigates the viability of the acetogenic strain *Eubacterium callanderi* KIST612 and its impact on acetate production across various operational modes. Unlike conventional single-reactor systems, a dual-reactor strategy was implemented to enhance viable cell retention, leading to improved process efficiency. This approach significantly increased the total carbon conversion rate to 9.30 mmol h^{-1} and the specific productivity of viable cells to 0.13 g $gcell^{-1}$ h^{-1} , ultimately achieving the highest acetate titer (34.4 g L^{-1}) with > 53 % cell viability. These findings represent a major advancement over previous studies, demonstrating that maintaining cell viability is critical for optimizing acetate productivity. By integrating viability control into process operations, this study presents a scalable and efficient strategy to enhance gas fermentation performance, improve substrate conversion efficiency, and expand biochemical production potential for industrial applications.

1. Introduction

Bioprocessing utilizes microbial metabolism to efficiently and sustainably convert raw materials into valuable products [1,2]. It aims to balance titer, rates, and yield (TRY metrics) while minimizing GHG emissions, ensuring industrial feasibility and environmental sustainability [3–5]. Syngas fermentation is a promising bioprocessing technique. Autotrophic organisms serve as alternatives for heterotrophic organism that ferment carbohydrate fermentation, for example. In this approach, instead of breaking down C5 or C6 sugar units, microbes build up C2-C6 products from C1 units, such as carbon monoxide or carbon dioxide [6]. Syngas, which primarily consists of CO, CO_2 and H_2 can be found in waste gases from heavy industries, such as steel mills, waste incineration plants, and refineries, or in synthesis gas generated from any biomass resource, such as unsorted and non-recyclable municipal solid waste or organic industrial waste. The sources of these C1 gases suggest that gas fermentation, which upcycles C1 units in waste gases using microbes, can be a more environmentally friendly and valuable technology compared to conventional chemical processes for waste gas treatment [7–9].

Acetogens are representative gas-fermenting bacteria that upcycle carbon oxides through the Wood-Ljungdahl pathway (WLP). Carbon dioxide is utilised as the starting material and is reduced to methyltetrahydrofolate (consuming one ATP) and carbon monoxide in the methyl and carbonyl branches of the WLP, respectively [10,11]. Because carbon monoxide is an intermediate in the WLP, many acetogens can utilise carbon oxides as both carbon and energy sources [12–14]. The produced methyltetrahydrofolate and carbon monoxide are condensed

* Corresponding author at: School of Environment and Energy Engineering, Gwangju Institute of Science and Technology, 123 Cheomdan-gwagiro, Buk-gu, Gwangju 61005, Republic of Korea.
E-mail address: ischang@gist.ac.kr (I.S. Chang).

https://doi.org/10.1016/j.jece.2025.116531
Received 10 February 2025; Received in revised form 10 March 2025; Accepted 5 April 2025
Available online 6 April 2025

into acetyl-CoA, a precursor of various metabolites and products (by acetyl-CoA synthase) [10,15]. Acetate can be generated from acetyl-CoA by securing one equivalent of ATP via two enzymatic reactions (using phosphotransacetylase and acetate kinase). Because of this ATP generation, most acetogens produce acetate as a single or major product during gas fermentation [16]. Although some acetogens can produce other chemicals (e.g. butyrate, ethanol, and butanol), the ATP yield per unit of syngas converted decreases as the metabolic pathways become more complex [17]. Acetate production is also industrially relevant, as acetate serves as a versatile platform chemical for producing various value-added products. The simplicity and efficiency of the acetate production pathway make it economically favourable for large-scale gas fermentation processes [18,19]. To date, several strains have been evaluated with the aim of enhancing the industrial capabilities in terms of metabolic efficiency and scalability, such as *Acetobacterium woodii*, *Clostridium autoethanogenum*, *Eubacterium callanderi*, *Moorella thermoacetica*, and *Sporomusa ovata* [20–23]. This study utilised *E. callanderi* KIST612, a methylotrophic acetogen known for its ability to effectively convert syngas into acetate via the Wood-Ljungdahl pathway [24]. Additionally, its metabolic versatility in converting C1 gas into various metabolites has been extensively studied, making it an ideal model strain for investigating the challenges of C1 gas utilisation and developing process-level strategies to overcome these limitations [21,25].

The utilisation of C1 gases to autotrophically produce C2-C6 compounds presents challenges compared to carbohydrate substrates, due to the need for synthesizing longer carbon chains. Despite the development of syngas fermentation leading to the operation of industrial plants, several areas still require improvement and further research, primarily due to the low carbon conversion rate, gas-liquid mass transfer and productivity associated with gas substrates [26]. To overcome these limitations, many studies have focused on increasing the biomass concentration to enhance process productivity. Various operational strategies, such as cell retention using external membranes and cell bleeding techniques, have been tested to secure higher biomass concentrations, which can lead to improved overall productivity [27,28]. Additionally, studies have shown that optimizing growth medium, gas mass transfer and process conditions resulted in higher productivity [29,30]. One of the commonly cited success factors of these studies is the improved microbial environmental conditions achieved through operational strategies. These strategies may have resulted in the retention of more viable cells and ultimately led to increased productivity. In previous studies, the cultivation of aerobic strains has been monitored in real time to assess cell viability, a critical parameter in bioprocess development. For instance, in a 10–15 mL working volume bioreactor, where glucose served as the primary substrate, viability was maintained at a maximum of 90 %, leading to the highest reported productivity of 16.2 g $cell^{-1}$ d^{-1} [31]. Additionally, in research employing non-thermal plasma treatment, cell viability was used as a key indicator to evaluate metabolic modifications and productivity improvements in adapted yeast strains. In such cases, viability has often been analysed as a secondary parameter to interpret bioprocess efficiency [32]. However, there remains a lack of comprehensive analysis on the extent to which the retained and expectedly increased number of viable cells is secured, and, more importantly, how these cells quantitatively contribute to the production of target compounds. Addressing this knowledge gap is essential for optimizing bioprocess strategies and enhancing fermentation performance in industrial applications. To address these knowledge gaps, we aimed to further investigate the impact of process operations on cell viability, product titer, and productivity. In this study, we analysed correlations between changes in process operations and cell viability in syngas fermentation to acetate. Modifying the process to maintain high viability of *E. callandri* should lead to improved TRY metrics.

2. Materials and methods

2.1. Cultivation of microbial strain and growth media

E. callanderi KIST612 was cultivated in a vial with a working volume of 60 mL, using a gas mixture of CO and CO_2 ($CO:CO_2 = 80:20$) at 1 atm and maintained at 37°C [25]. The cells were cultured in carbonate-buffered basal medium (CBBM), which included yeast extract, L-cysteine, $NaHCO_3$, basal medium, trace element solution, and 0.1 % resazurin solution. Additionally, 1 % sodium phosphate (prepared from 1 mol L^{-1} NaH_2PO_4 and 0.5 mol L^{-1} Na_2HPO_4) and 1 % vitamin solution were added to the vial for cultivation as shown in Table S2 [33].

2.2. Reactor setup and operating conditions

Custom-designed bubble column reactors (BCRs) with capacities of 4 L (Reactor 1; working volume of 3 L) and 500 mL (Reactor 2; working volume of 0.35 L) were employed for gas fermentation [34,35]. Reactor 1 was used for producing viable cells, while the Reactor 2 was for accumulating these cells. The set-up and operating conditions are shown in Fig. 1 and operation modes are described in Table 1. In all modes (single-stage and two-stage), the gas substrates were continuously supplied. The CO and CO_2 gas mixtures ($CO:CO_2 = 80:20$ and $CO:CO_2 = 90:10$) were supplied by Daedeok Gas (Republic of Korea) and introduced into the gas recirculation line (10 mL min^{-1}) through a flow meter (Kofloc, Japan). The CO to CO_2 ratio was selected based on prior studies to minimize limiting conditions [21,33,34]. Since CO is the primary carbon source for *Eubacterium callanderi*, a low CO ratio could lead to rapid depletion of dissolved CO, affecting microbial activity. Given the fixed reactor design, CO-rich conditions were initially used, and in the final mode, the CO ratio was increased to 90 % to assess its impact. The mixed gas in the recirculation line was introduced in the reactor through a sintered gas filter with a pore size of 10–16 μm (Daihan Science, Republic of Korea). This gas inflow ranging from 0.06 to 0.86 vvm (volume of mixed gas per volume of liquid per minute). The pH was controlled at 7.0, which is known to be the optimal condition for acetate production by *E. callanderi* KIST612, by adding 2 mol L^{-1} NaOH through a control unit (R3610, Consort, Belgium). Different operational modes were applied using as growth medium SFM (sludge filtrate medium), CBBM or 8XCBBM (Table S2). The fresh growth medium was replaced using dilution rates (D; h^{-1}) ranging from 0.012 to 0.018 h^{-1}. The dilution rate was determined based on our previous studies [21,29,33], where growth limitations under the current medium recipe were identified. Accordingly, the medium concentration was increased while the dilution rate was gradually reduced across operational modes. To obtain samples for product analysis, outflowing fermentation broth was filtered using a hollow-fibre membrane cartridge (CFP-2-E-3MA, GE Healthcare, USA) connected to Reactor 2. Except for the outflowing fermentation broth, the cells and broth continuously circulated (30 mL min^{-1}) between the reactor and the hollow fiber membrane [21]. During the S1 operation, the medium broth containing microorganisms was transferred from Reactor 1 to Reactor 2 (Fig. 1) once the cell concentration in Reactor 1 reached 0.1–0.2 g L^{-1} (S1). Following cell accumulation, the operation switched to S2 mode in Reactor 2, employing an 8X concentrated CBBM with a dilution rate of 0.018 h^{-1} and a gas flow rate of 0.69 vvm. The growth medium was prepared in a 5-L glass vessel, autoclaved at 121°C for 20 minutes, and purged with the same gas composition used in the gas fermentation process. The vessel was connected with a 10-L gas bag filled with the same gas ($CO:CO_2 = 80:20$ and $CO:CO_2 = 90:10$) while continuously supplying growth medium into the reactor.

2.3. Analytical methods

Biomass and liquid samples were collected at 1 mL per sampling time from the liquid sampling point. The dry cell concentration C_x was determined by measuring absorbance at 600 nm using a UV–vis

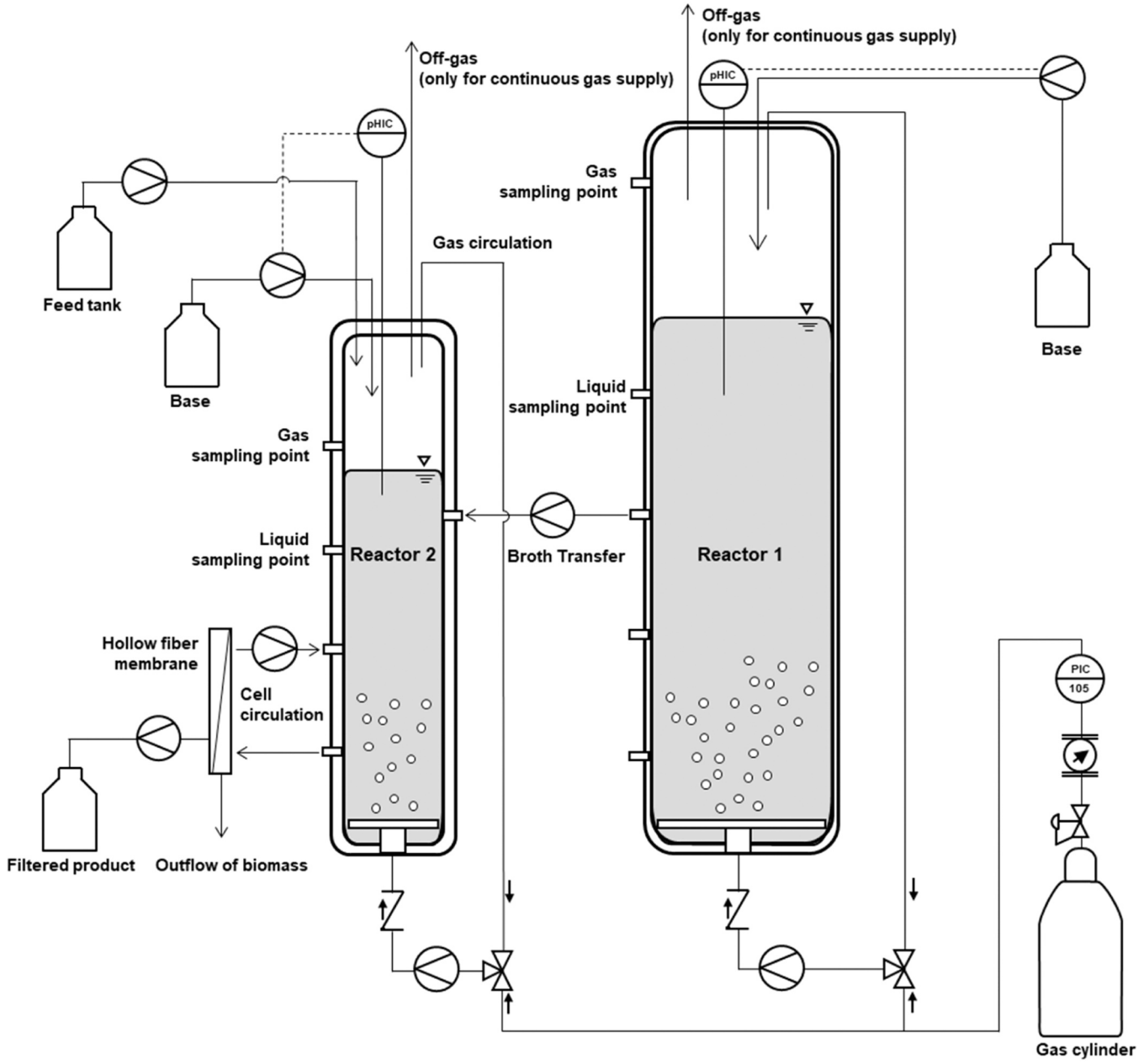

Fig. 1. Schematic diagram of cell accumulated gas fermentation reactor operation. Reactor 1 for viable cell growth, Reactor 2 for cell accumulation.

spectrophotometer (V-730, JASCO, MD, USA). The total biomass concentration was calculated by multiplying the measured OD value by a conversion factor of 0.27 $g_{X,total}$ OD^{-1} [25]. The gas was sampled using a 100 µl sample lock syringe (Hamilton, Schweiz). Gas composition was analysed with a gas chromatograph (GC; ACME 6100, Young Lin Instrument Co., Korea) equipped with a thermal conductivity detector (TCD). To separate the gas components, a carbon molecular sieve column (Carboxen 1000, 60/80 mesh, Supelco, Park, Bellefonte, PA, USA) was used in the oven. Liquid metabolites were analysed using a gas chromatograph (GC; ACME 6000, Young Lin Instrument Co.) fitted with a flame ionization detector (FID). A capillary column (AquaWax, Alltech, Deerfield, IL, USA) was used to separate chemical species in the oven. The injector temperature was maintained at 250°C with a flow rate of 2.0 mL min^{-1} .

2.4. Definition of viable cells and dye staining for cell viability

In this study, 'viable cells' are not defined as a strict distinction between fully live and dead cells, but as microorganisms exhibiting high levels of activity. The analysis of viability was conducted based on the proportion of highly viable cells by using PI (propidium iodide) and CFDA (carboxyfluorescein diacetate) staining, where CFDA indicates viable cells by emitting green fluorescence, and PI stains non-viable cells by emitting red fluorescence. A PI solution was prepared by dissolving it in distilled water to achieve a final concentration of 0.5 mg mL^{-1}. A CFDA solution was prepared by dissolving 9 mg in a mixture of 1 mL DMSO (dimethyl sulfoxide) and 9 mL distilled water, resulting in a final concentration of 0.9 mg mL^{-1}. Both solutions were stored in a refrigerator [36–38]. To ensure the accuracy of the viability measurements for *E. callanderi* KIST612, all processes were conducted in a glove box under N_2 condition to avoid damage by oxygen. The OD of the samples was measured at 600 nm, and the samples were diluted based on an OD of

Table 1
Operation condition of *E. callanderi* KIST612.

Name of Operation	Reactor	Growth medium		Gas substrate		
		Mode	Type	$CO:CO_2$	vvm	mL min^{-1}
Batch	R2	Batch	CBBM	80:20	0.06–0.69	21–240
Continuous	R2	Continuous $D = 0.018\ h^{-1}$ Cell circulation 27 mL min^{-1}	CBBM	80:20	0.69	240
Titer production mode (Table S3)	R2	Continuous $D = 0.012\ h^{-1}$ Cell circulation 27 mL min^{-1}	8X CBBM	80:20	0.69	240
S1	R1	Batch (Transfer the fermentation broth to R2)	CBBM	80:20	-	240
	R2	Continuous (Accumulating fermentation broth from R1)	CBBM	80:20	0.69	240
S2	R2	Continuous $D = 0.018\ h^{-1}$	8X CBBM	80:20	0.69	240
S3	R2	Continuous $D = 0.018\ h^{-1}$	SFM	80:20	0.69–0.86	240–300
S4	R2	Continuous $D = 0.018\ h^{-1}$	SFM	90:10	0.86	300

0.83 for flow cytometry (CyFlow, Partec, Japan). The samples and dyes were mixed in a 2:1:1 vol ratio (sample:PI:CFDA) and incubated in the dark at 37 °C for 15 min for staining (Fig. S1).

2.5. Calculation of specific productivity

The volume-specific productivity r_p (g $L^{-1}h^{-1}$) was calculated using the following equations:

$$V_L\frac{dC_P}{dt} = \quad Q_{in}C_{P,in} - Q_{out}C_P - r_P V_L \tag{1}$$

Where $C_{P,in}$ represents the initial concentration of the product, V_L represents the working volume, and Q_{in} represents medium flow rate (L h^{-1}).

Volumetric productivity can be derived by integrating Eq. (1) as follows (Equation S1- S10):

$$r_P = \quad \frac{D(C_{t1} - e^{D\Delta t} \times C_{t2})}{1 - e^{D\Delta t}} \tag{2}$$

where C_t represents the product concentration (g L^{-1}) at time t, and Δt is the difference between sampling time that measure the product concentration.

The total biomass-specific productivity $q_{P,total}$(g_P $g_{X,total}^{-1}$ h^{-1}) was calculated using Eq. (3).

$$q_{P,total} \quad = \frac{r_P}{C_{X,total}} \tag{3}$$

The viable biomass concentration ($C_{X,viable}$), specific growth rate (μ, h^{-1}) and viable biomass-specific productivity of viable cells ($q_{P,active}$, g_P $g_{X,viable}^{-1}$ h^{-1}) was calculated according to Eq. (4), Eq. (5) and Eq. (6), where v represents cell viability (%) Since a membrane is used in the system, no cell outflow occurs.

.

$$C_{X,viable} = \frac{C_{X,total}}{v} \tag{4}$$

$$\mu = \frac{1}{C_X}\frac{dC_X}{dt} \tag{5}$$

$$q_{P,viable} \quad = \frac{r_P}{C_{X,viable}} \tag{6}$$

2.6. Statistical Analysis

The correlation coefficient was calculated using the Pearson's correlation coefficient equation:

$$r_{XY} = \quad \frac{\sum_i^n (X_i - \overline{X})(Y_i - \overline{Y})}{\sqrt{\sum_i^n (X_i - \overline{X})^2}\sqrt{\sum_i^n (Y_i - \overline{Y})^2}} \tag{7}$$

where r_{XY} represents correlation coefficient, X_i represents values of the variable X, and $\overline{X}$ represents average of variables.

3. Results and discussion

3.1. Cell viability in different operation modes in gas fermentation

Cell viability and total biomass concentration were assessed during gas fermentation in a single bioreactor (Reactor 2) to elucidate the differences between various operational modes, as shown in Fig. 2. For the initial three days, the bioreactor was operated in batch mode with a continuous gas supply. During this period, the total biomass concentration increased linearly to 0.78 g L^{-1} , while cell viability declined to 40 %, possibly due to nutrient limitations associated with early stage batch-mode operation. A similar rapid decline has been observed in other strains under batch and fed-batch conditions, suggesting that one or more operational factors act as limiting constraints, reducing cell viability [39,40]. Upon transitioning to continuous medium supply, the total biomass concentration increased gradually to 0.95 g L^{-1} and the cell viability increased to 73 %. This increase in viability appears to be a result of the accelerated viable cell growth and cell performance due to the additional nutrients provided by the continuous mode. As the biomass concentration gradually increased to 1.21 g L^{-1} (0.85 g L^{-1} of viable biomass concentration), the higher cell density let to an increased demand for nutrients and gases. Consequently, the viability did not improve further and gradually decreased. At day 8, although no steady state had been achieved considering the cell concentration, it was confirmed that viability remained stable. To observe changes under these conditions, the operation mode was shifted from continuous mode to titer production mode (Table 1). This change involved reducing the dilution rate to 0.012 h^{-1} and increasing the concentration of the growth medium (8X CBBM). The total biomass concentration increased to 3 g L^{-1} but the viable biomass concentration remained in the range of 0.85 ± 0.13 g L^{-1} as cell viability declined to 24 %. Although transitioning to continuous medium supply initially boosted viability and biomass concentration, the increasing demand for nutrients and gases as

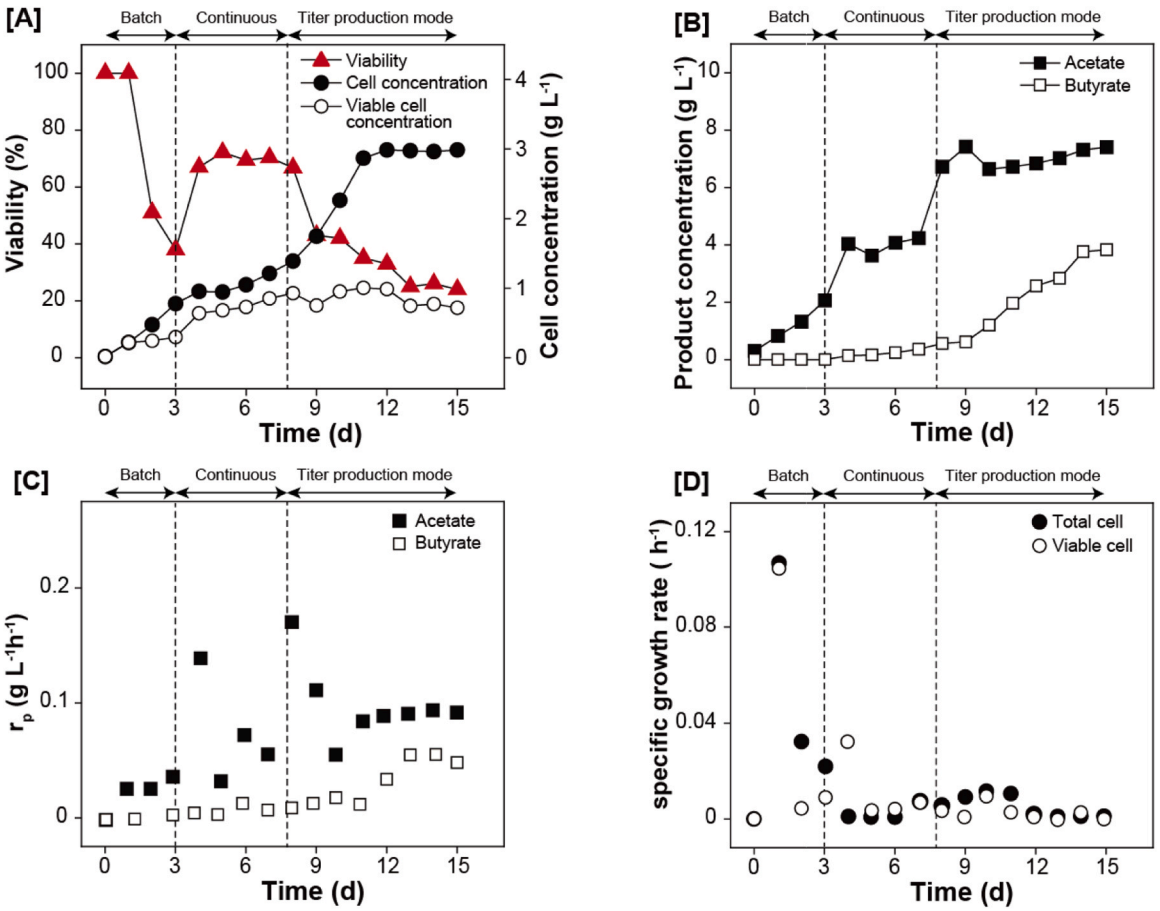

Fig. 2. The performance of cell viability [A], product concentration [B], volume-specific productivity [C] and specific growth rate [D] at time series for R2 as a single-reactor operation.

biomass grew led to a gradual decline in cell viability. This decline can be attributed to the accumulation and coexistence of both high- and low-viability cells throughout the process. This suggests that additional operational strategies are needed to sustain high cell viability over extended fermentation periods.

3.2. Evaluating acetate and butyrate production

As shown in Fig. 2**(B) and (C)**, the concentration of acetate changed at different operation modes, and the productivity temporarily increased right after each change. However, volume-specific productivity eventually stabilised, maintaining an average of 0.048 ± 0.018 g L^{-1} h^{-1} between days 5 and 7 and 0.086 ± 0.005 g L^{-1} h^{-1} between days 11 and 15. During this period, the total biomass concentration continued to increase, while the concentration of viable biomass remained relatively constant (Fig. 2**(A)**). This is also evident in the specific growth rate for each operation mode, where the total cell concentration steadily increased, but increase in viable biomass concentration was only observed at the start of the operation ($\mu_{X,total}$: 0.106 h^{-1} and $\mu_{X,viable}$: 0.105 h^{-1}) and when switching to continuous mode ($\mu_{X,total}$: 0.021 h^{-1} and $\mu_{X,viable}$: 0.032 h^{-1}) (Fig. 2**(D)**). These results can be explained using either one of two hypotheses. The first suggests that total biomass concentration is correlated with acetate productivity, where prolonged process times and increased cell density result in lower productivity per cell. The second hypothesis posits that acetate productivity aligns more closely with viable cell density than with total cell density. In this case, the actual productivity per cell would remain relatively unchanged from day 5–15, leading to stable overall productivity.

To evaluate which of these hypotheses is more plausible, specific productivity was assessed in relation to both total cell concentration ($q_{p,total}$; Fig. 3**(A)**) and viable biomass concentration ($q_{p,viable}$; Fig. 3**(B)**) under different operational modes (batch, continuous, and titer production). At high cell concentrations, a lower $q_{p,total}$ of acetate was observed. Each operation mode exhibits $q_{p,total}$ higher than 0.1 g_p $g_{x,total}^{-1}$ h^{-1} at a single point (Fig. 3**(A)**). However, this increase was temporary, resulting from transient variations in inflow gas velocity or medium composition. Notably, the $q_{p,total}$ at a total cell concentration of 3 g L^{-1} (0.03 $g_{x,total}^{-1}$ h^{-1}) in the titer production mode was lower than that observed in the batch mode operation (0.04 $g_{x,total}^{-1}$ h^{-1}) at cell concentrations lower than 0.5 $g_{x,total}$ L^{-1}. The observed reduction in $q_{p,total}$ at higher biomass concentrations was not solely due to a decrease in the efficiency of individual cells caused by limited conditions. In addition to the decrease in productivity per cell, the concentration of viable cells remained within a similar range (0.82 ± 0.11 g L^{-1}, as indicated by the dashed line in Fig. 3**(B)**) compared to the total cell concentration (2.03 ± 0.90 g L^{-1}). This suggests that the changes in overall acetate production are not primarily caused by a decrease in cell productivity when the total cell concentration increases. Thus, maintaining a high viable cell concentration is as crucial as ensuring sufficient per-cell productivity.

In contrast, butyrate production commenced when low viability (< 45 %) was observed (Fig. 2**(B)**). The main product produced by the cells remains acetate but, the butyrate production starts under conditions of reduced cell viability. This observation confirms that (Fig. 3**(C)**), at higher cell concentrations, acetate productivity decreases, and butyrate formation either begins or results from excess acetate through chain elongation [41]. However, when normalized by the viable cell concentration, the specific productivity of acetate increased, even though

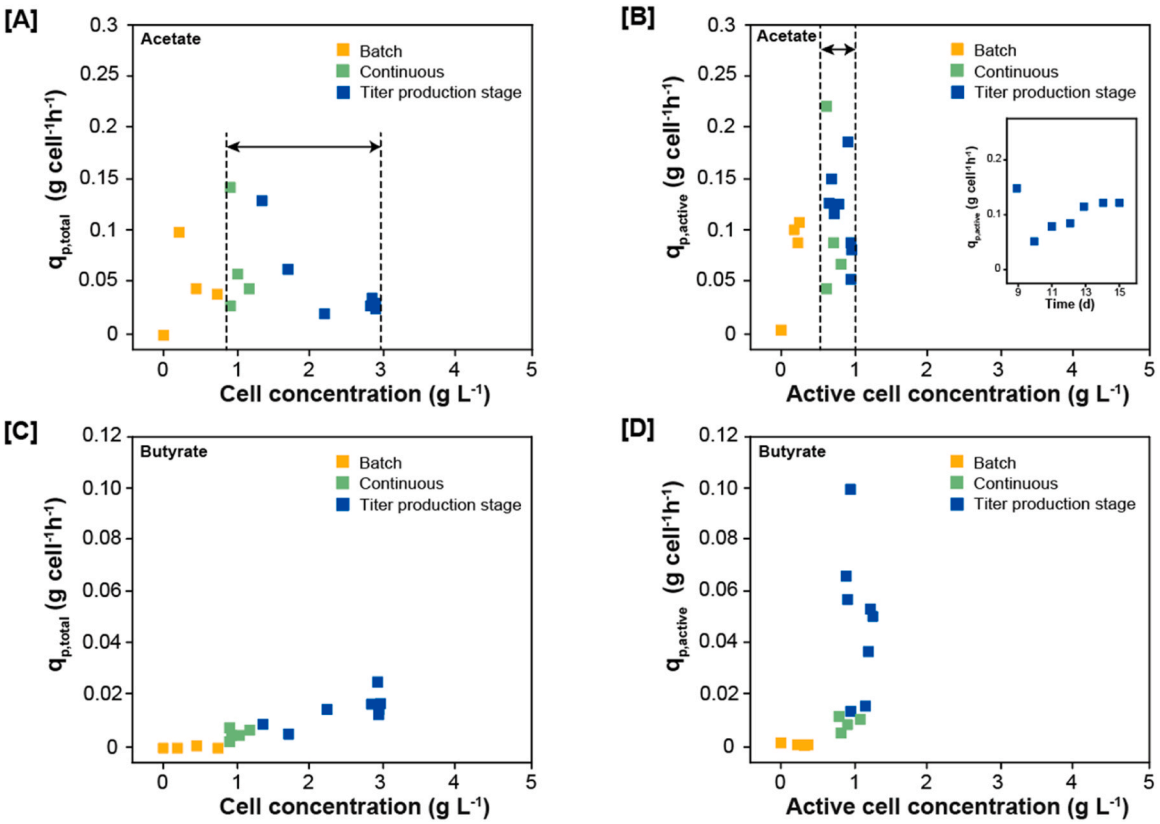

Fig. 3. Specific productivity of acetate [A, B] and butyrate [C, D] across cell and viable cell concentrations in different operational modes at R2 as a single reactor operation. The dashed line indicates the range of cell concentration variation during the continuous and titer production stages.

butyrate production increased. (Fig. 3**(B) and (D)**).

It is known that each microbe has a specific maximum productivity per cell, but the exact maximum values for various target products and conditions have not yet been clearly measured. Consequently, previous strategies have involved increasing the total biomass concentration via the use of biomass accumulation or other strategy to enhance the overall process productivity [27,34,42]. However, the results of our study suggest that rather than merely increasing cell density, it is crucial to provide conditions that enhance biomass specific productivity while maintaining a high concentration of viable cells. This approach maximises acetate productivity in our study.

3.3. Enhancing product titer by maintaining high cell viability

Given these findings, it becomes clear that maintaining highly viable *E. callanderi* KIST612 is thus critical for producing high concentrations of acetate. Furthermore, viability rapidly declines under limited culture conditions, highlighting the importance of optimising the nutrient supply and gas flow for sustained microbial activity and product yield [43,44].

As shown in Fig. 4**(A)**, the cell concentration in S1 increased from 4.76 to 8.19 g L^{-1} over 3 days, with an average viability of 69.6 ± 1.4 % and 23 % CO utilisation. When accumulation ceased in S2 (with R1 turned off), the process stabilised, maintaining a viability of 63.3 ± 1.6 % and 25 % CO utilisation. Cells continued to consume CO to sustain ATP production, resulting in a stable transition to the stationary phase. In S3, to increase the acetate concentration and maintain viability, the system was switched to an SFM (sludge filtrate medium) that had previously achieved maximum acetate production with the same strain and system [33]. Additionally, on day 12, the gas flow rate was increased to 0.86 vvm to enhance CO substrate supply. During the S2-S3 period, the cell concentration remained constant at 8.73 ± 0.16 g L^{-1} , while viability decreased to 56.3 %. Despite this reduction in viability, when compared to a single-reactor operation using the same gas concentration and flow (Fig. 2), the total cell concentration was 2.9 times higher, and viability was 2.3 times greater, resulting in a 6.9-fold increase in the number of viable cells. This high retention of viable cells enabled us to achieve an acetate concentration of 27.3 g L^{-1} with 34 % CO utilisation in S3 (Fig. 4**(B)**), which is 1.79 times higher than the process operation using the same medium in S3 reported in a previous paper (cell concentration of 7.2 g L^{-1} and maximum acetate production of 15.2 g L^{-1}) [33]. The significant impact of retaining viable cells was evident, as evidenced by the enhanced system productivity (Table 2**)**. In the S4 stage, the CO ratio in the input gas composition was increased from 80 % to 90 % to enhance the supply of carbon monoxide. This resulted in a final cell concentration of 8.64 g L^{-1} (with a viable cell concentration of 4.59 g L^{-1} at 53 % viability), achieving a maximum acetate concentration of 34.4 g L^{-1} and an acetate productivity of 0.72 g L^{-1} h^{-1} , with 40 % CO utilisation.

Implementation of strategies at each stage effectively minimised the reduction in cell viability after securing a high cell concentration. Consequently, there was no significant difference in specific productivity between the total and viable cell concentrations during the S2 and S3 stages. However, as the operating time and CO concentration increased in S4, although the cell concentration remained relatively constant, the specific productivity increased, leading to a noticeable difference (Fig. 4**(C)**). In summary, from S2 to S4, following the concentration process, the total cell concentration remained at 8.68 g L^{-1} , while the conversion rate of CO to product increased by 85 % for acetate (from 3.79 mmol h^{-1} to 7.03 mmol h^{-1}) and 61 % for butyrate (from 1.41 mmol h^{-1} to 2.27 mmol h^{-1}). Moreover, the specific CO conversion rate, based on cell viability, increased by 126 % for acetate (1.53 mmol h^{-1}) and 97 % for butyrate (0.50 mmol h^{-1}) as shown in Fig. 4**(D)**. This outcome underscores the effectiveness of a process

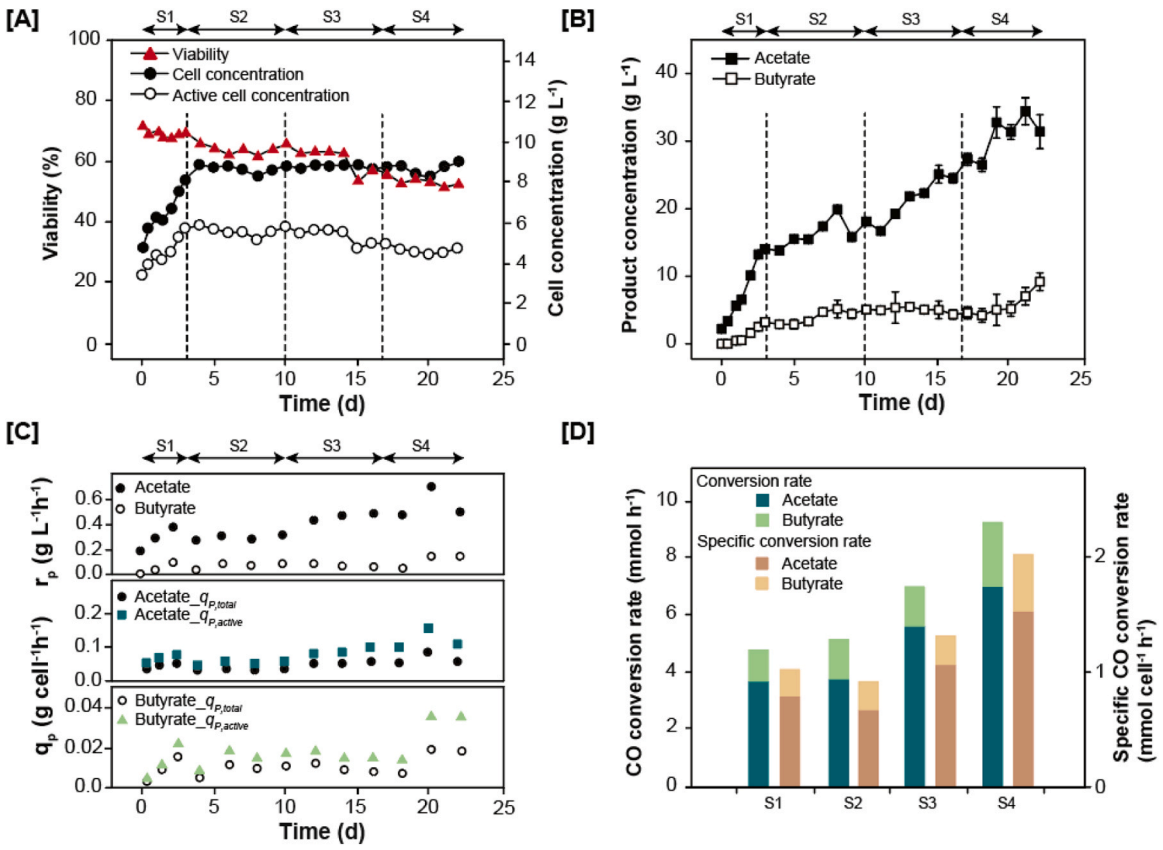

Fig. 4. Operation profile at R2 (S1-S4) of biomass [A], product concentration [B], specific productivity [C], and CO conversion rate and specific CO conversion rate (calculated by viable cell concentration) [D] in cell accumulation mode for securing viable cell in different operational stages (S1-S4).

Table 2
Acetate productivity and biomass concentration of *E. callanderi* KIST612 under different operation modes.

Operation mode	Biomass ($g\ L^{-1}$)	Productivity ($g\ L^{-1}\ h^{-1}$)	Reference
Continuous (stage 5)	5.02	0.16	Lee et al. [21]
Mixed feeding (stage 3)	5.79	0.16	Lee et al. [21]
Mixed feeding	5.78	0.22	Lee et al., [31]
Viable cell accumulation (S1)	5.69	0.24	Current paper
Mixed feeding	7.23	0.24	Lee et al., [31]
Viable cell accumulation (S3)	8.80	0.45	Current paper
Viable cell accumulation (S4)	8.64	0.59	Current paper

operation strategy that considers cell viability, necessitating a more detailed analysis of productivity in relation to viable cell concentration.

3.4. Biomass specific productivity of *E. callanderi KIST612*

Comparing the productivity between this study and previous studies, it appears that the overall system productivity increased as the total cell concentration increased (Fig. 5**(A)**). Specifically, in this study, an 89 % increase of the total cell concentration from 4.7 g L^{-1} to 8.9 g L^{-1} resulted in a volume-specific productivity increase of 75 %. Additionally, while it may seem that productivity increased as the total cell concentration is maintained between S2 and S4, a detailed analysis of cell viability (Fig. 5**(B)**) revealed that viable cell concentration decreased. However, productivity improved due to the operational strategy employed (Fig. S2). This operational strategy, which involves an optimised nutrient and gas supply, likely enhanced metabolic efficiency and reduced stress conditions, thereby improving specific productivity.

If specific productivity were only analysed using the total cell concentration (Fig. 4**(C) and** Fig. 5**(C)**), it can be observed that specific productivity increased from 0.03 to 0.09 g L^{-1} h^{-1} , while cell concentration remained stable between 8.2 and 8.9 g L^{-1} . Based on these data, one might assume that maximum specific productivity had nearly been reached and that increasing cell density should be the primary focus. However, the changes in the operational conditions proposed in this study successfully maintained a higher proportion of viable cells compared with a single reactor, thereby increasing the ratio of cells participating in acetate production. Although the concentration of viable cells decreased by 20 % from 5.9 g L^{-1} to 4.7 g L^{-1} , specific productivity increased by 50 % from 0.06 g L^{-1} h^{-1} to 0.09 g L^{-1} h^{-1} .

Interestingly, when analysing specific productivity based on viable cells, the single reactor operation exhibited a higher maximum specific productivity of 0.22 g L^{-1} h^{-1} compared to S1-S4 (Fig. 5**(D)**). This can be attributed to the fact that, during the process of concentrating microorganisms to secure viable cells in a short period, the maximum viability achieved was 72 %, whereas in the single reactor, higher viability was secured during the exponential phase at lower cell concentrations. However, the absolute difference in the viable cell concentration resulted in a significant difference in overall acetate production. The average $q_{p,viable}$, during the stationary phase of the single reactor (between days 12 and 15) was 0.10 ± 0.02 $g_{acetate}$ $cell^{-1}$ h^{-1} , while the average $q_{p,viable}$ in S4 was 0.13 ± 0.03 $g_{acetate}$ $cell^{-1}$ h^{-1} , reflecting a 30 % difference. When calculated based on the volume-specific productivity, the difference was even more pronounced, with the single reactor showing 0.03 ± 0.01 $g_{acetate}$ $cell^{-1}$ h^{-1} compared to 0.07 ± 0.02 $g_{acetate}$ $cell^{-1}$ h^{-1} in S4, demonstrating a 130 % difference.

High cell density was achieved through careful control of the dilution rates and substrate availability, which minimised cell death and maximised metabolic activity. Simultaneously, by establishing an operational strategy that maintains high specific productivity, this study achieved

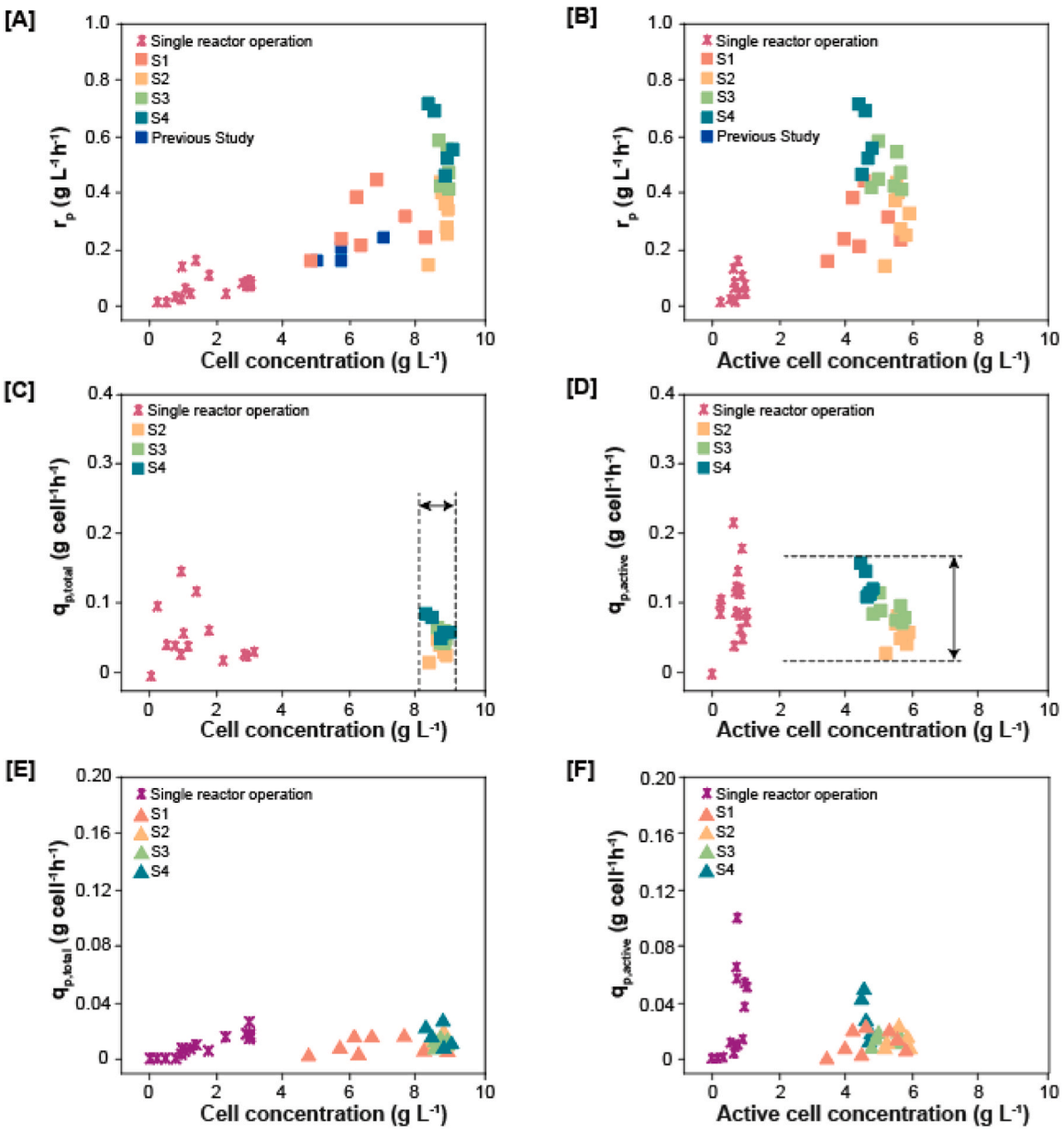

Fig. 5. The productivity ([A] and [B]) and specific productivity ([C] and [D]) of acetate and specific productivity ([E] and [F]) of butyrate in *Eubacterium callanderi* KIST612 at different cell concentrations across different operation stages (S1–S4).

the highest acetate product concentration reported thus far for the *E. callanderi* KIST612 strain (34.4 g L^{-1}). In another study conducted with *Acetobacterium woodii*, improvements in stirring conditions led to enhanced acetate production, even though the biomass levels decreased [45]. This highlights the significant influence that both cell activity and environmental conditions can have on overall productivity, demonstrating that productivity gains do not solely depend on cell concentration, but also on how well operational conditions are optimised to support cell activity.

Interestingly, this trend was not observed for butyrate. The specific productivity of butyrate, aside from an increase in S4, remained relatively constant regardless of cell concentration (Fig. 5**(E) and (F)**). In the case of S4, the increase in specific productivity was attributed to a higher CO ratio, which increased the amount of carbon source and electron donor, indicating that the viable cell ratio had a minimal impact on butyrate productivity. This confirms that in acetogens, acetate production is the most efficient and straightforward process, with a short pathway for ATP generation, leading to an immediate increase in productivity as cell activity increases [16]. However, butyrate production, requiring a more complex pathway and higher NADH levels, must be evaluated through a more intricate correlation [46].

3.5. *A perspective on viable cell as a key performance indicator in bioprocess engineering*

To compare how viability is definitively reflected as a major indicator in bioprocessing, correlation coefficients were calculated for viability, viable cell concentration, and other relevant factors (Fig. 6**(A) and** Table S1-S5). According to the data obtained in this study, cell viability decreased as the process progressed. However, owing to process operation strategies aimed at minimising the reduction in viability and increasing titer productivity, a negative correlation was observed. Moreover, the correlation was stronger $q_{p,viable\_acetate}$ (-0.74 and −0.76) than $q_{p,total\_acetate}$ (-0.61 and −0.63). This indicates that an analysis method that accounts for viability, along with strategies for securing highly viable cells, has a significant impact on process evaluation and

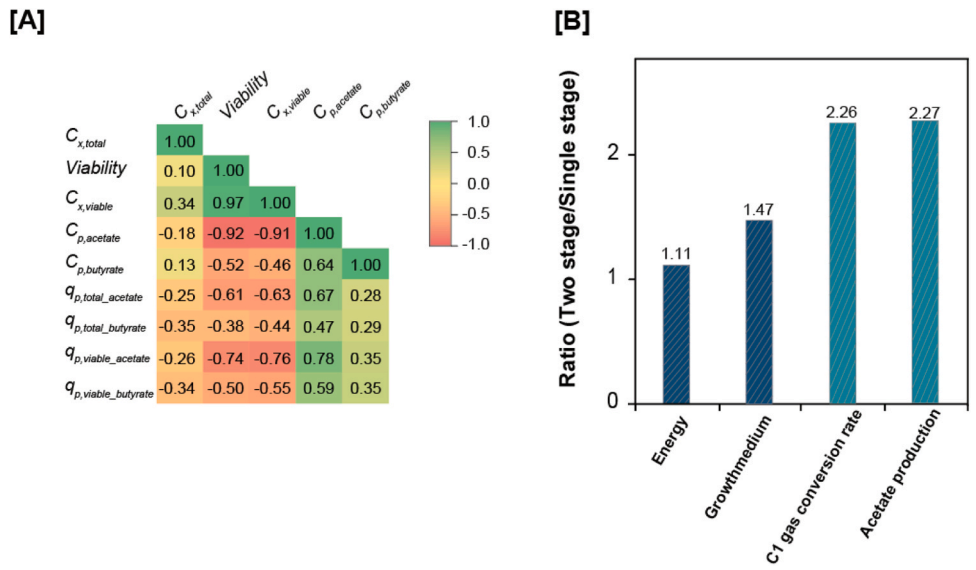

Fig. 6. Correlation analysis of viable cell accumulation mode in two-stage operation (S2-S4) in this study [A]. Ratio comparison between different operation modes: viable cell accumulation (two-stage) and MC-SGCR (single-stage) in gas fermentation [B].

productivity enhancement when assessing acetate productivity in bioprocesses.

The highly viable cell-securing strategy used in this study involved operating a two-stage reactor to ensure a high concentration of viable cells at the beginning of the process. However, this approach has several limitations, particularly in terms of resource consumption and economic feasibility. As shown in Fig. 6**(B)**, this method requires 1.1 times more electrical energy and 1.5 times more growth medium, leading to increased operational costs and resource demand, especially in large-scale applications. Additionally, the necessity for extra reactors and process complexity during the initial phase may pose engineering and scalability challenges, making implementation less practical for industrial settings with strict cost and infrastructure constraints. However, this is justified as it enables a 2.26-fold increase in the C1 gas conversion rate and a 2.27-fold increase in acetate production within the same timeframe. Furthermore, because the additional inputs during the initial operation remain constant, the differences in energy and medium consumption decrease as the production period is extended, enhancing the operational stability. Therefore, conducting a full TEA (Techno Economic Analysis) and LCA (Life Cycle Assessment) would be beneficial to further validate the feasibility and sustainability of this approach.

Viability is a crucial parameter that must be considered in gas fermentation processes and should be integrated into operational strategies to maintain high cell activity and enhance acetate productivity. Further research is required to establish appropriate viability levels to produce long-chain chemicals. While operational strategies are typically based on the characteristics of microorganisms and actual data, most experiments have analysed microbial populations by averaging their overall behaviour [47]. However, individual cells exhibit differences in their metabolic capabilities and productivity. Therefore, future research should focus on precisely evaluating cell viability at the single-cell level, rather than relying solely on population-averaged analyses.

4. Conclusion

This study demonstrated the critical importance of maintaining cell viability when optimising the gas fermentation process for acetate production using *Eubacterium callanderi* KIST612. By adopting operational strategies aimed at enhancing cell viability, we not only enhanced the total carbon conversion rate by 106 % (9.30 mmol h^{-1}) but also achieved the highest reported acetate concentration of 34.4 g L^{-1} compared to previous studies. This outcome underscores the necessity of tailoring the process conditions to enhance cell activity (>53 % of cell viability), thereby improving overall productivity and process stability. These findings highlight that prioritising cell viability can lead to significant advancements in the efficiency and feasibility of gas fermentation systems. This research provides a strong foundation for further exploration of viability-based approaches to produce not only acetate but also other valuable chemicals from C1 gases. Additionally, as the demand for sustainable and economically viable bioprocesses continues to grow, the strategies developed in this study can be applied broadly across various industrial applications, offering a pathway for more environmentally friendly production methods. Furthermore, as individual cells exhibit differences in their capabilities and productivity, more precise studies that consider cell viability at the single-cell level. This approach is essential for optimising overall performance, as addressing variability among cells will allow for even greater control and enhancement of the fermentation processes. Additionally, refining operational strategies and explore their applicability in the production of long-chain carbon compounds, further enhancing the industrial potential of gas fermentation technologies.

CRediT authorship contribution statement

Lee Mungyu: Writing – original draft, Visualization, Validation, Investigation, Formal analysis, Data curation. **Ji Nulee:** Resources, Investigation. **Kim Ji-Yeon:** Validation, Investigation. **Straathof Adrie J.J.:** Writing – review & editing. **Jourdin Ludovic:** Writing – review & editing. **Chang In Seop:** Writing – review & editing, Funding acquisition.

Declaration of Competing Interest

The authors declare that they have no competing financial interests or personal relationships that may have influenced the work reported in this study.

Acknowledgements

This study was supported by grants from the National Research Foundation of Korea (NRF), funded by the Korean government (NRF-2015M3D3A1A01064883 and NRF-2021R1A5A1028138).

Appendix A. Supporting information

Supplementary data associated with this article can be found in the online version at doi:10.1016/j.jece.2025.116531.

Data Availability

Data will be made available on request.

References

[1] O. Cabau-Peinado, M. Winkelhorst, R. Stroek, R. de Kat Angelino, A.J. Straathof, K. Masania, J.M. Daran, L. Jourdin, Microbial electrosynthesis from CO2 reaches productivity of syngas and chain elongation fermentations, Trends Biotechnol. (2024).

[2] K. Boodhoo, M. Flickinger, J. Woodley, E. Emanuelsson, Bioprocess intensification: a route to efficient and sustainable biocatalytic transformations for the future, Chem. Eng. Process. -Process. Intensif. 172 (2022) 108793.

[3] J.M. Clomburg, A.M. Crumbley, R. Gonzalez, Industrial biomanufacturing: the future of chemical production, Science 355 (6320) (2017) aag0804.

[4] M. Lee, C.N. Reddy, B. Min, In situ integration of microbial electrochemical systems into anaerobic digestion to improve methane fermentation at different substrate concentrations, Int. J. Hydrog. Energy 44 (4) (2019) 2380–2389.

[5] R.R. Singhania, A.K. Patel, A. Singh, D. Haldar, S. Soam, C.-W. Chen, M.-L. Tsai, C.-D. Dong, Consolidated bioprocessing of lignocellulosic biomass: technological advances and challenges, Bioresour. Technol. 354 (2022) 127153.

[6] T. Janković, A.J. Straathof, A.A. Kiss, Advanced downstream processing of bioethanol from syngas fermentation, Sep. Purif. Technol. 322 (2023) 124320.

[7] J. Li, J. Tseng, D. Tang, Y. Yong, L. Sun, Y.-X. Huo, Upcycling C1 gas-derived resources in future food system, Resour., Conserv. Recycl. 210 (2024) 107827.

[8] C. Zhang, R. Fu, L. Kang, Y. Ma, D. Fan, Q. Fei, An upcycling bioprocess for sustainable aviation fuel production from food waste-derived greenhouse gases: life cycle assessment and techno-economic analysis, Chem. Eng. J. 486 (2024) 150242.

[9] R.M. Handler, D.R. Shonnard, E.M. Griffing, A. Lai, I. Palou-Rivera, Life cycle assessments of ethanol production via gas fermentation: anticipated greenhouse gas emissions for cellulosic and waste gas feedstocks, Ind. Eng. Chem. Res. 55 (12) (2016) 3253–3261.

[10] H.L. Drake, Acetogenesis, acetogenic bacteria, and the acetyl-CoA "Wood/Ljungdahl" pathway: past and current perspectives, Acetogenesis (1994) 3–60.

[11] V. Müller, Energy conservation in acetogenic bacteria, Appl. Environ. Microbiol. 69 (11) (2003) 6345–6353.

[12] J. Abrini, H. Naveau, E.-J. Nyns, Clostridium autoethanogenum, sp. nov., an anaerobic bacterium that produces ethanol from carbon monoxide, Arch. Microbiol. 161 (1994) 345–351.

[13] T.D. Allen, M.E. Caldwell, P.A. Lawson, R.L. Huhnke, R.S. Tanner, Alkalibaculum bacchi gen. nov., sp. nov., a CO-oxidizing, ethanol-producing acetogen isolated from livestock-impacted soil, Int. J. Syst. Evolut. Microbiol. 60 (10) (2010) 2483–2489.

[14] B. Jiang, A.-M. Henstra, P.L. Paulo, M. Balk, W. van Doesburg, A.J. Stams, Atypical one-carbon metabolism of an acetogenic and hydrogenogenic Moorella thermoacetica strain, Arch. Microbiol. 191 (2009) 123–131.

[15] S.W. Ragsdale, E. Pierce, Acetogenesis and the Wood–Ljungdahl pathway of CO2 fixation, Biochim. Et. Biophys. Acta (BBA)-Proteins Proteom. 1784 (12) (2008) 1873–1898.

[16] J.-Y. Kim, M. Lee, S. Oh, B. Kang, M. Yasin, I.S. Chang, Acetogen and acetogenesis for biological syngas valorization, Bioresour. Technol. 384 (2023) 129368.

[17] J. Bertsch, V. Müller, Bioenergetic constraints for conversion of syngas to biofuels in acetogenic bacteria, Biotechnol. Biofuels 8 (2015) 1–12.

[18] C. Liu, G. Luo, W. Wang, Y. He, R. Zhang, G. Liu, The effects of pH and temperature on the acetate production and microbial community compositions by syngas fermentation, Fuel 224 (2018) 537–544.

[19] B.M. Harahap, B.K. Ahring, Acetate production from syngas produced from lignocellulosic biomass materials along with gaseous fermentation of the syngas: a review, Microorganisms 11 (4) (2023) 995.

[20] H. Kang, B. Park, N.R. Bolo, D. Pathiraja, S. Park, M. Cha, I.G. Choi, I.S. Chang, Gene-centric metagenome analysis reveals gene clusters for carbon monoxide conversion and validates isolation of a clostridial acetogen for C2 chemical production, Biotechnol. J. 14 (6) (2019) 1800471.

[21] M. Lee, M. Yasin, N. Jang, I.S. Chang, A simultaneous gas feeding and cell-recycled reaction (SGCR) system to achieve biomass boosting and high acetate titer in microbial carbon monoxide fermentation, Bioresour. Technol. 298 (2020) 122549.

[22] F.E. Liew, R. Nogle, T. Abdalla, B.J. Rasor, C. Canter, R.O. Jensen, L. Wang, J. Strutz, P. Chirania, S. De Tissera, Carbon-negative production of acetone and isopropanol by gas fermentation at industrial pilot scale, Nat. Biotechnol. 40 (3) (2022) 335–344.

[23] F. Rahayu, Y. Kawai, Y. Iwasaki, K. Yoshida, A. Kita, T. Tajima, J. Kato, K. Murakami, T. Hoshino, Y. Nakashimada, Thermophilic ethanol fermentation from lignocellulose hydrolysate by genetically engineered Moorella thermoacetica, Bioresour. Technol. 245 (2017) 1393–1399.

[24] J. Jeong, J.-Y. Kim, B. Park, I.-G. Choi, I.S. Chang, Genetic engineering system for syngas-utilizing acetogen, Eubacterium limosum KIST612, Bioresour. Technol. Rep. 11 (2020) 100452.

[25] I.S. Chang, B.H. Kim, R.W. Lovitt, J.S. Bang, Effect of CO partial pressure on cell-recycled continuous CO fermentation by Eubacterium limosum KIST612, Process Biochem. 37 (4) (2001) 411–421.

[26] M. Köpke, S.D. Simpson, Pollution to products: recycling of 'above ground'carbon by gas fermentation, Curr. Opin. Biotechnol. 65 (2020) 180–189.

[27] L. Perret, N. Boukis, Jr Sauer, Influence of increased cell densities on product ratio and productivity in syngas fermentation, Ind. Eng. Chem. Res. 62 (35) (2023) 13799–13810.

[28] H. Richter, M.E. Martin, L.T. Angenent, A two-stage continuous fermentation system for conversion of syngas into ethanol, Energies 6 (8) (2013) 3987–4000.

[29] N. Jang, M. Yasin, M. Lee, H. Kang, I.S. Chang, Gas circulation rate and medium exchange ratio as influential factors affecting ethanol production in carbon monoxide fermentation using a packed-bed reactor, Sustain. Energy Fuels 4 (4) (2020) 1963–1973.

[30] K. Asimakopoulos, H.N. Gavala, I.V. Skiadas, Reactor systems for syngas fermentation processes: a review, Chem. Eng. J. 348 (2018) 732–744.

[31] S. Rameez, S.S. Mostafa, C. Miller, A.A. Shukla, High-throughput miniaturized bioreactors for cell culture process development: Reproducibility, scalability, and control, Biotechnol. Prog. 30 (3) (2014) 718–727.

[32] N. Recek, R. Zhou, R. Zhou, V.S.J. Te'o, R.E. Speight, M. Mozetič, A. Vesel, U. Cvelbar, K. Bazaka, K. Ostrikov, Improved fermentation efficiency of S. cerevisiae by changing glycolytic metabolic pathways with plasma agitation, Sci. Rep. 8 (1) (2018) 8252.

[33] M. Lee, N. Jang, B. Kang, M. Yasin, J.-Y. Kim, I.S. Chang, Proposition of cost-effective industrial grade medium for synthesis gas fermentation through evaluation of economic feasibility, Bioresour. Technol. Rep. 19 (2022) 101208.

[34] J.-H. Kim, M. Lee, H. Jeong, S. Ko, S.-H. Moon, I.S. Chang, Recycling of minerals with acetate separation in biological syngas fermentation with an electrodialysis system, Chem. Eng. J. 459 (2023) 141555.

[35] N. Jang, M. Yasin, H. Kang, Y. Lee, G.W. Park, S. Park, I.S. Chang, Bubble coalescence suppression driven carbon monoxide (CO)-water mass transfer increase by electrolyte addition in a hollow fiber membrane bioreactor (HFMBR) for microbial CO conversion to ethanol, Bioresour. Technol. 263 (2018) 375–384.

[36] L.L. Chan, A.R. Wilkinson, B.D. Paradis, N. Lai, Rapid image-based cytometry for comparison of fluorescent viability staining methods, J. Fluoresc. 22 (5) (2012) 1301–1311.

[37] S. Fan, Z. Xiao, Y. Zhang, X. Tang, C. Chen, W. Li, Q. Deng, P. Yao, Enhanced ethanol fermentation in a pervaporation membrane bioreactor with the convenient permeate vapor recovery, Bioresour. Technol. 155 (2014) 229–234.

[38] J. Kolek, B. Branska, M. Drahokoupil, P. Patakova, K. Melzoch, Evaluation of viability, metabolic activity and spore quantity in clostridial cultures during ABE fermentation, FEMS Microbiol. Lett. 363 (6) (2016) fnw031.

[39] P.A. Apostolidis, A. Tseng, M.-E. Koziol, M.J. Betenbaugh, B. Chiang, Investigation of low viability in sparged bioreactor CHO cell cultures points to variability in the Pluronic F-68 shear protecting component of cell culture media, Biochem. Eng. J. 98 (2015) 10–17.

[40] U.M. Lim, M.G.S. Yap, Y.P. Lim, L.-T. Goh, S.K. Ng, Identification of autocrine growth factors secreted by CHO cells for applications in single-cell cloning media, J. Proteome Res. 12 (7) (2013) 3496–3510.

[41] S. Park, M. Yasin, J. Jeong, M. Cha, H. Kang, N. Jang, I.-G. Choi, I.S. Chang, Acetate-assisted increase of butyrate production by Eubacterium limosum KIST612 during carbon monoxide fermentation, Bioresour. Technol. 245 (2017) 560–566.

[42] N. Jang, M. Lee, M. Yasin, I.S. Chang, Behavior of CO-water mass transfer coefficient in membrane sparger-integrated bubble column for synthesis gas fermentation, Bioresour. Technol. 311 (2020) 123594.

[43] H.N. Abubackar, F.R. Bengelsdorf, P. Dürre, M.C. Veiga, C. Kennes, Improved operating strategy for continuous fermentation of carbon monoxide to fuel-ethanol by clostridia, Appl. Energy 169 (2016) 210–217.

[44] J.R. Phillips, R.L. Huhnke, H.K. Atiyeh, Syngas fermentation: a microbial conversion process of gaseous substrates to various products, Fermentation 3 (2) (2017) 28.

[45] F. Steger, L. Rachbauer, M. Windhagauer, L.F. Montgomery, G. Bochmann, Optimisation of continuous gas fermentation by immobilisation of acetate-producing Acetobacterium woodii, Anaerobe 46 (2017) 96–103.

[46] A. Katsyv, V. Müller, Overcoming energetic barriers in acetogenic C1 conversion, Front. Bioeng. Biotechnol. 8 (2020) 621166.

[47] M.S. Pino, R.M. Rodríguez-Jasso, M. Michelin, A.C. Flores-Gallegos, R. Morales-Rodriguez, J.A. Teixeira, H.A. Ruiz, Bioreactor design for enzymatic hydrolysis of biomass under the biorefinery concept, Chem. Eng. J. 347 (2018) 119–136.